

Supporting Information for

The Oxidation of Cysteine by Electrogenenerated Hexacyanoferrate (III) in Microliter Droplets

Kathryn J. Vannoy^a, Jeffrey E. Dick^{a,b*}

^aDepartment of Chemistry, The University of North Carolina at Chapel Hill, Chapel Hill, NC 27599, USA

^bLineberger Comprehensive Cancer Center, School of Medicine, The University of North Carolina at Chapel Hill, Chapel Hill, NC 27599, USA

*To whom correspondence should be addressed: jedick@email.unc.edu

Table of Contents

| | |
|---|--------|
| pH considerations (Figure S1) | S2 |
| Other voltammetry for bulk rate determination (Figure S2)..... | S3 |
| Other micrographs and voltammetry for confined rate determination (Figure S3) | S4-5 |
| Discussion of error in contact radius measurement (Figure S4) | S6 |
| COMSOL simulation for apparent rate constant (Figure S5-7, Tables S1-3)..... | S7-11 |
| COMSOL simulation for adsorption (Figure S8-9, Table S4)..... | S12-17 |
| References..... | S18 |

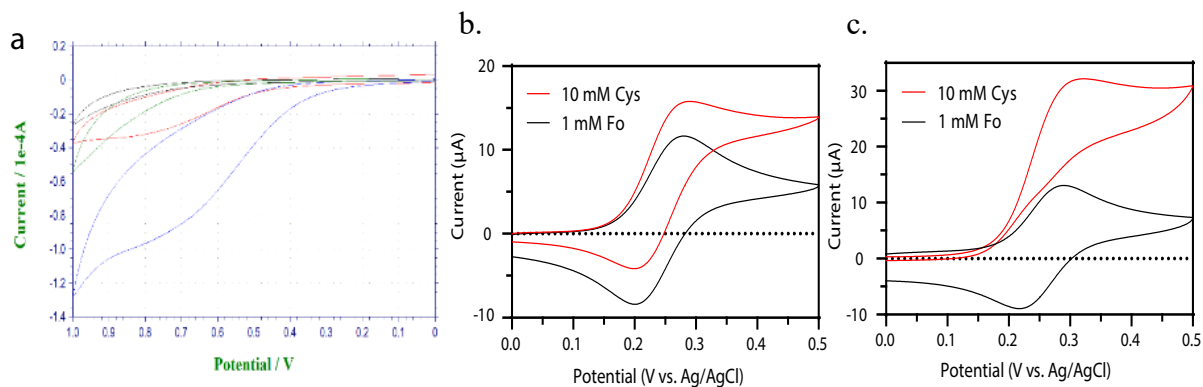


Figure S1. (a) Overlaid cyclic voltammograms for the electrochemical oxidation of 10 mM cysteine at various pH. Electrochemical responses from lowest oxidizing potentials to highest: (blue) 10 mM cysteine in 1 M NaOH (pH = 14), (red) 10 mM cysteine in 50 mM phosphate buffer, 0.5 mM KCl (pH = 6.4), and (red) 10 mM cysteine in 1 mM HCl, 0.4 mM KCl (pH = 3). In this panel, the scan rate was 0.05 V/s and the anodic current is represented as negative, in line with polarographic convention. **(b)** Cyclic voltammogram of 1 mM hexacyanoferrate (II) with (red) and without (black) 10 mM cysteine in 1 mM HCl (pH = 3). **(c)** Cyclic voltammogram of 1 mM hexacyanoferrate (II) with (red) and without (black) 10 mM cysteine in 10 mM phosphate buffer, 1 M KCl (pH = 6.4). For panels b-c, the scan rate was 0.05 V/s and in line with IUPAC convention the anodic current is plotted positive. For all voltammograms in this figure, three electrodes were used: working, reference, and counter electrode of glassy carbon, Ag/AgCl, and platinum wire coil, respectively.

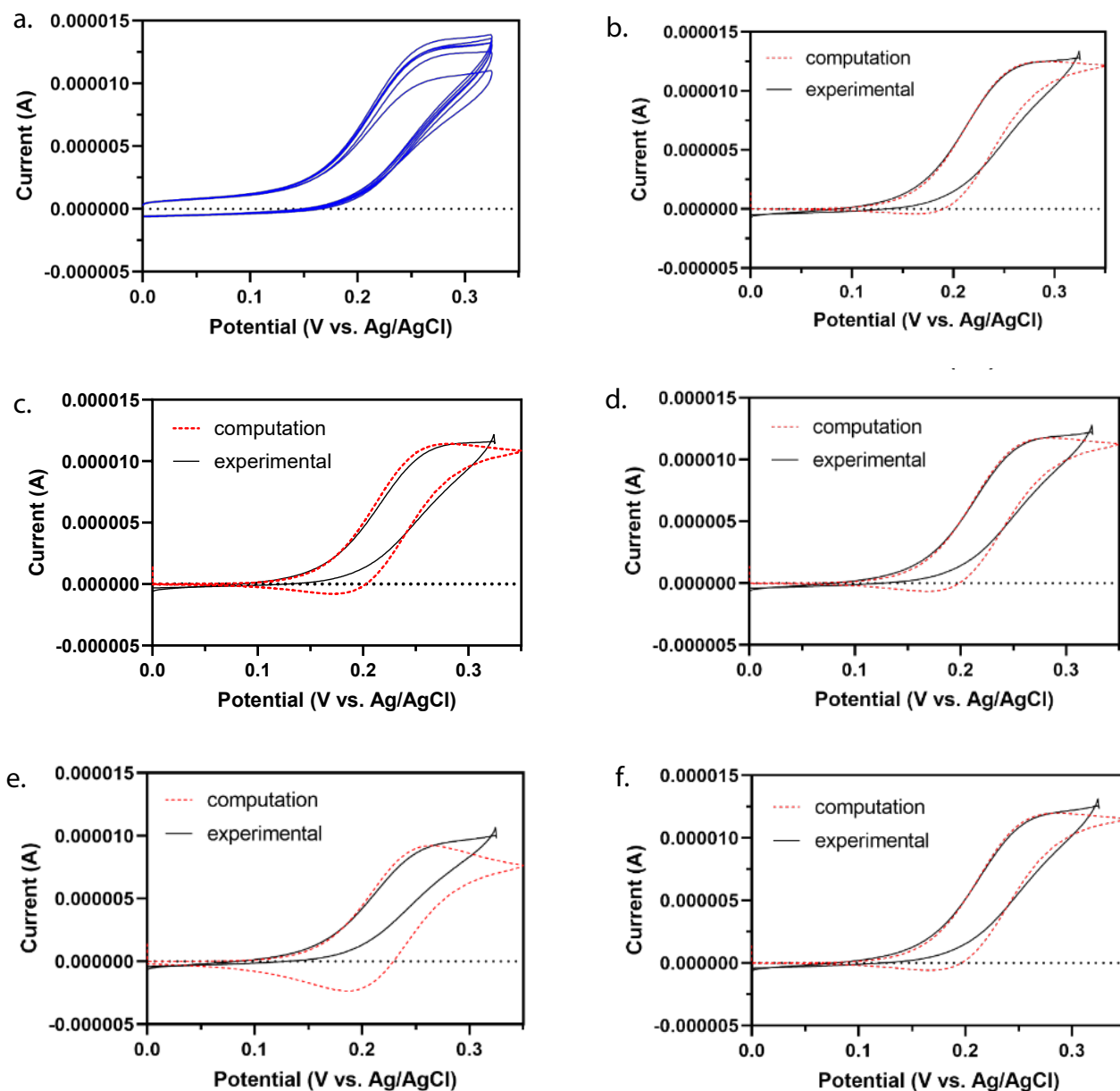
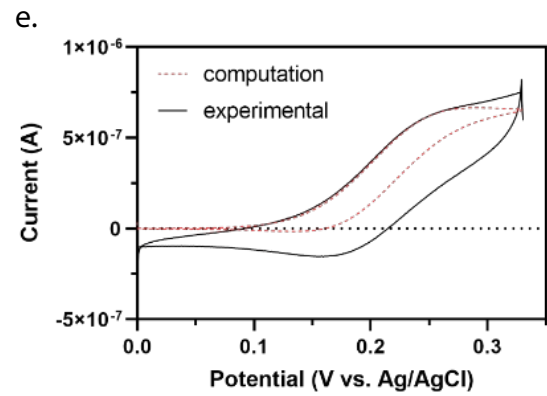
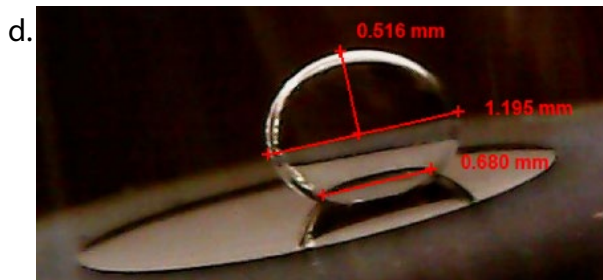
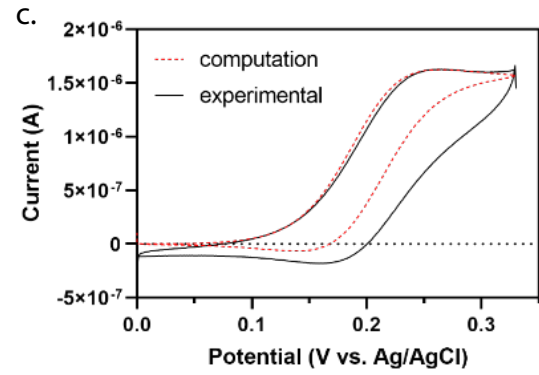
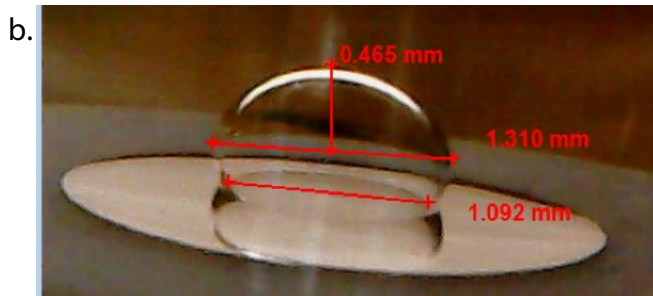
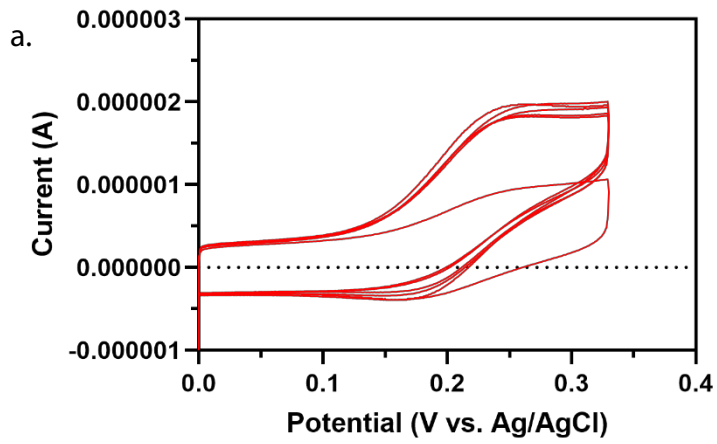


Figure S2. (a) All experimental cyclic voltammograms obtained using the prepared bulk solution of 0.5 mM hexacyanoferrate (II) and 5 mM cysteine in 50 mM phosphate buffer and 0.5 M KCl (pH = 6.3) including the raw experimental data shown in Figure 3a. Each full scan (start/end potential = 0 V vs. Ag/AgCl) represents a different measurement in the same solution. All six experimental cyclic voltammograms were fit and used for the bulk kinetic analysis shown in Figure 3h. (b-f) Additional fits that are represented in the bulk kinetic analysis in Figure 3h. The scan rate for all voltammetry was 0.1 V/s and in line with IUPAC convention the anodic current is plotted as positive. For all experimental voltammograms, three electrodes were used: working, reference, and counter electrode of glassy carbon, Ag/AgCl, and platinum wire coil, respectively.



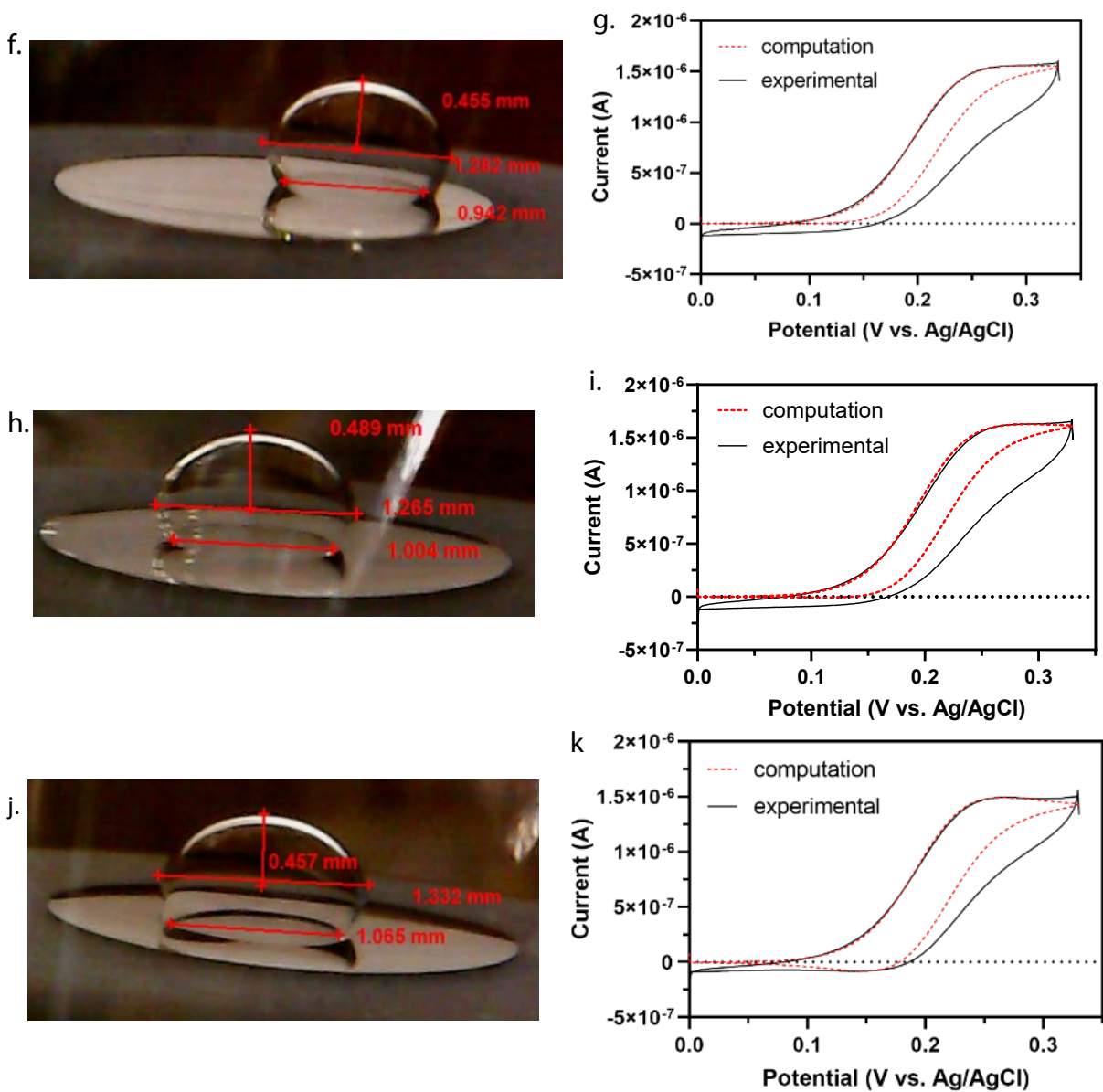


Figure S3. (a) All cyclic voltammograms obtained in 1 μL droplets using the prepared bulk solution of 0.5 mM hexacyanoferrate (II) and 5 mM cysteine in 50 mM phosphate buffer and 0.5 M KCl (pH = 6.3) including the raw experimental data shown in Figure 3e. Each full scan (start/end potential = 0 V vs. Ag/AgCl) represents a different measurement in the same solution. (b-k) Rows of additional micrographs and the corresponding fit for used for the droplet kinetic analysis in Figure 3h. The scan rate for all experiments was 0.1 V/s and in line with IUPAC convention the anodic current is plotted as positive. For all experimental voltammograms, three electrodes were used: working, reference, and counter electrode of glassy carbon, Ag/AgCl, and platinum wire coil, respectively.

Error in the contact measurement for a droplet can propagate significant error in the calculated kinetic parameter, as shown in the rather large error bars in Figure 3h. To quantify this error, we measured an image with an unclear contact (see image in Figure S6h) 10 times and fit the data by using the maximum, minimum and average measured droplet contact to inform the simulation geometry, calculating k_c values of $690 \text{ M}^{-1}\text{s}^{-1}$, $810 \text{ M}^{-1}\text{s}^{-1}$, and $735 \text{ M}^{-1}\text{s}^{-1}$, respectively. In our experiments, the focal plane of the video microscope will dictate our certainty in the contact radius. This error is exacerbated by the limiting pixel width ($8 \mu\text{m}$) of the video microscopy.

| | Length |
|----|--------|
| 1 | 0.917 |
| 2 | 0.948 |
| 3 | 0.938 |
| 4 | 0.943 |
| 5 | 0.928 |
| 6 | 0.922 |
| 7 | 0.942 |
| 8 | 0.922 |
| 9 | 0.932 |
| 10 | 0.937 |

Figure S4. 10 measurements of the contact diameter using ImageJ software.

COMSOL Simulation to Determine the Apparent Rate Constant ($k_{c,app}$).

COMSOL Multiphysics 5.5 was used to fit experimental data to simulation. The geometry was built by a 2D-axisymmetric model, where the solution was defined as a 90° sector angle of an ellipse (see elaboration in next section). For bulk solutions the ellipse radii (r_{height} and r_{width}) were set at 10 cm. For droplet-confined geometries the optically measured height, width and contact of each droplet was specified for each simulation.

The electroanalysis physics module was used, where Electroanalytical Butler-Volmer equations described the heterogenous kinetics and cyclic voltammetry boundary conditions were selected through the electrode surface settings. The homogenous bimolecular reaction was described by additional physics (chemistry), where the rate of change for each species involved in the chemical reaction was described as shown below:

$$\text{Reaction rate}_{\text{hexacyanoferrate (II)}} = k_c[\text{hexacyanoferrate (III)}][\text{cysteine}]$$

$$\text{Reaction rate}_{\text{hexacyanoferrate (III)}} = -k_c[\text{hexacyanoferrate (III)}][\text{cysteine}]$$

$$\text{Reaction rate}_{\text{cysteine}} = k_c[\text{hexacyanoferrate (III)}][\text{cysteine}]$$

$$\text{Reaction rate}_{\text{cystine}} = -k_c[\text{hexacyanoferrate (III)}][\text{cysteine}]$$

Table S1. Parameters that remained constant throughout all computations for the bulk experiments.

| | |
|--|---|
| Hexacyanoferrate (II) diffusion coefficient ¹ | 6.5 x 10 ⁻¹⁰ m ² /s |
| Hexacyanoferrate (III) diffusion coefficient | 6.5 x 10 ⁻¹⁰ m ² /s |
| Cysteine diffusion coefficient ² | 1 x 10 ⁻⁹ m ² /s |
| Cystine diffusion coefficient ³ | 5 x 10 ⁻⁹ m ² /s |
| Heterogenous rate constant (k^0) | 0.001 m/s |
| Electrode radius | 0.0015 m |
| Solution radius (width) | 0.1 m |
| Solution radius (height) | 0.1 m |
| Domain maximum mesh size | 1 x 10 ⁻² m |
| Boundary maximum mesh size (along electrode surface) | 5 x 10 ⁻⁵ m |
| Point maximum mesh size (outer rim of electrode) | 5 x 10 ⁻⁶ m |
| Hexacyanoferrate (III) initial concentration | 0 mM |
| Cystine initial concentration | 0 mM |
| Equilibrium potential | 0.225 |
| Transfer coefficient | 0.5 |

To match specific experimental conditions, the following parameters were changed: the initial concentrations of hexacyanoferrate (II) and cysteine, the start, vertex and end potentials for voltammetry, and the scan rate.

The bulk model was altered for the droplet-confined experiments and was compared to an experimental voltammogram of 1 mM hexacyanoferrate (III) (Figure S6). The droplet simulation has the following changes:

Table S2. The droplet simulation has the following changes from the bulk model.

| | |
|--|--------------------------|
| Solution radius (width) | Determined by microscopy |
| Solution radius (height) | Determined by microscopy |
| Solution contact/electrode surface | Determined by microscopy |
| Domain maximum mesh size | 4×10^{-5} m |
| Boundary maximum mesh size (along electrode surface) | 1×10^{-6} m |
| Point maximum mesh size (outer rim of electrode) | 1×10^{-7} m |
| Equilibrium potential | 0.205 |

Table S3. The additional parameters when including the proton and buffering species reactions.

| Name | Expression/Value | Description |
|--------|---|--|
| HPO42- | 50 [mM] | Concentration of buffer base |
| H2PO4- | 50 [mM] | Concentration of buffer acid |
| D_PO4 | 6×10^{-10} [m ² /s] ⁴ | Diffusion coefficient buffer species |
| D_H | 7.8×10^{-9} [m ² /s] ⁵ | Diffusion coefficient of hydronium |
| K2 | 6.2×10^{-8} | Dissociation constant phosphate buffer |

$H_2PO_4^- \xrightleftharpoons{K2} H^+ + HPO_4^{2-}$ is defined as an equilibrium reaction in the chemistry physics

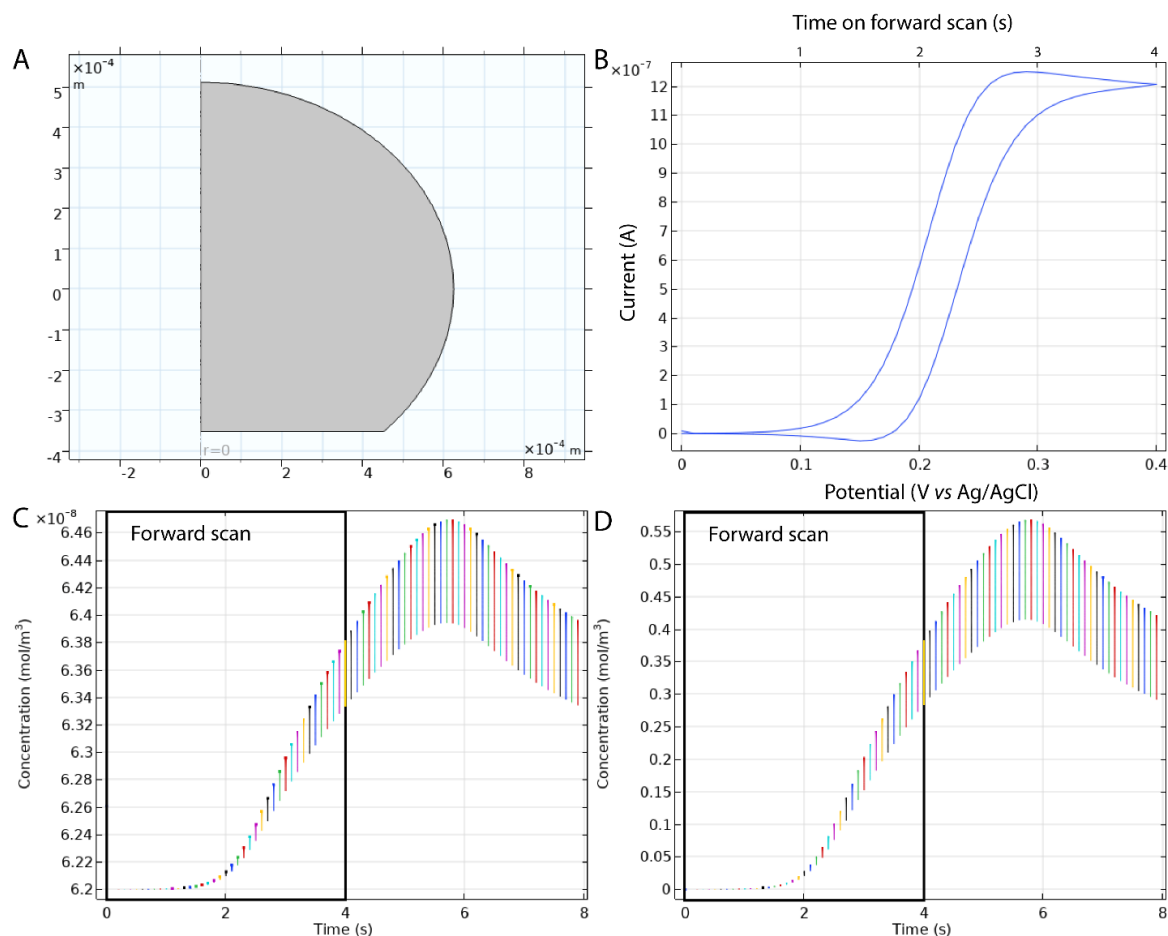


Figure S5. (A) 2D-axisymmetric geometry (B) Simulated voltammetry (0.1 V/s) for the reaction of 0.5 mM hexacyanoferrate (II) and 5 mM cysteine in 50 mM phosphate buffer. The $k_{c,app}$ was described as the average value, $490 \text{ M}^{-1}\text{s}^{-1}$. (C) Plot of the released proton concentration at the electrode surface over the voltammetry experiment. (D) Plot of cystine at the electrode surface over the voltammetry experiment. For Panels C and D, the entire electrode is probed, and the different concentration values for each time point show the variability on different points of the electrode. For both species, the highest concentrations at each time point correspond to the point in the center of the droplet and the lowest concentrations for each time point correspond to the edge of the droplet.

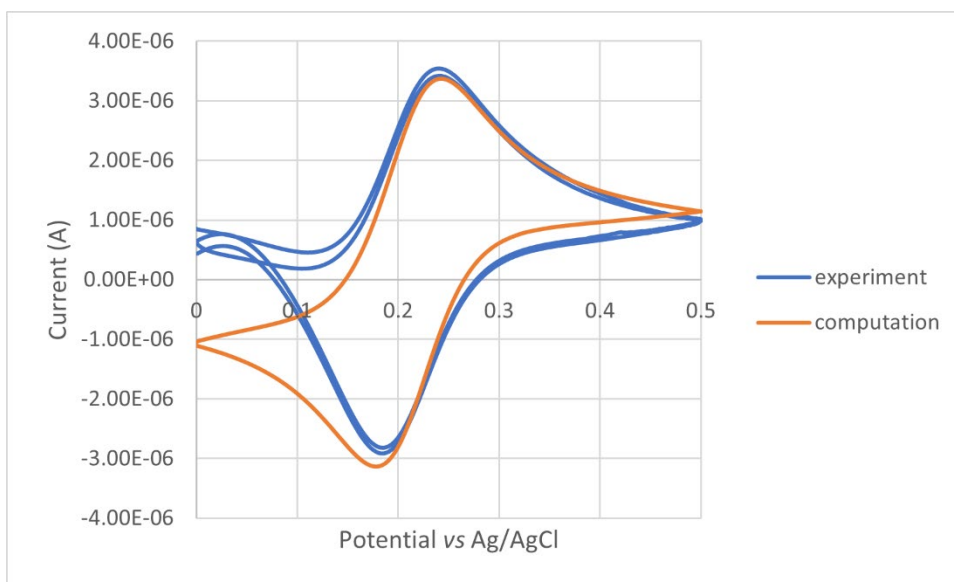


Figure S6. Computational fit (orange) overlaid with an experimental cyclic voltammogram (blue) of 1 mM ferrocyanide and 50 mM phosphate buffer (pH = 6.3) in 0.5 M KCl. A platinum working electrode, Ag/AgCl reference electrode, and platinum wire counter electrode were used (scan rate 0.1 V/s). The experimental voltammetry was background subtracted, and the shape from 0-0.1 V vs Ag/AgCl occurs due to the subtraction of oxygen reduction. In line with the IUPAC convention, anodic current is plotted as positive.

When fitting computation to either bulk or droplet experimental voltammetry, the only adjustable parameter was the rate constant, k_c . The droplet height, width, and contact angle do not have a significant influence on the simulated voltammetry. In contrast, the contact radius has a big influence on the simulated voltammetry. Figure S7a-c shows three 2D axisymmetric simulations, where the contact radius is changed to explore the range seen in the measured images. Figure S7d shows an overlay of the resulting simulations for a reaction of 1 mM hexacyanoferrate (II) and 10 mM cysteine, where the k_c was set to $500 \text{ M}^{-1}\text{s}^{-1}$. Figure S7e-g illustrates the effect on the local concentration of hexacyanoferrate (III) for the observed range of k_c values for the droplet geometry depicted in Figure S7b. With faster k_c values the hexacyanoferrate (III) is consumed quickly, and the concentration gradient stays closer to the electrode surface. Figure S7h shows the simulated voltammograms for the range of k_c values determined in droplets.

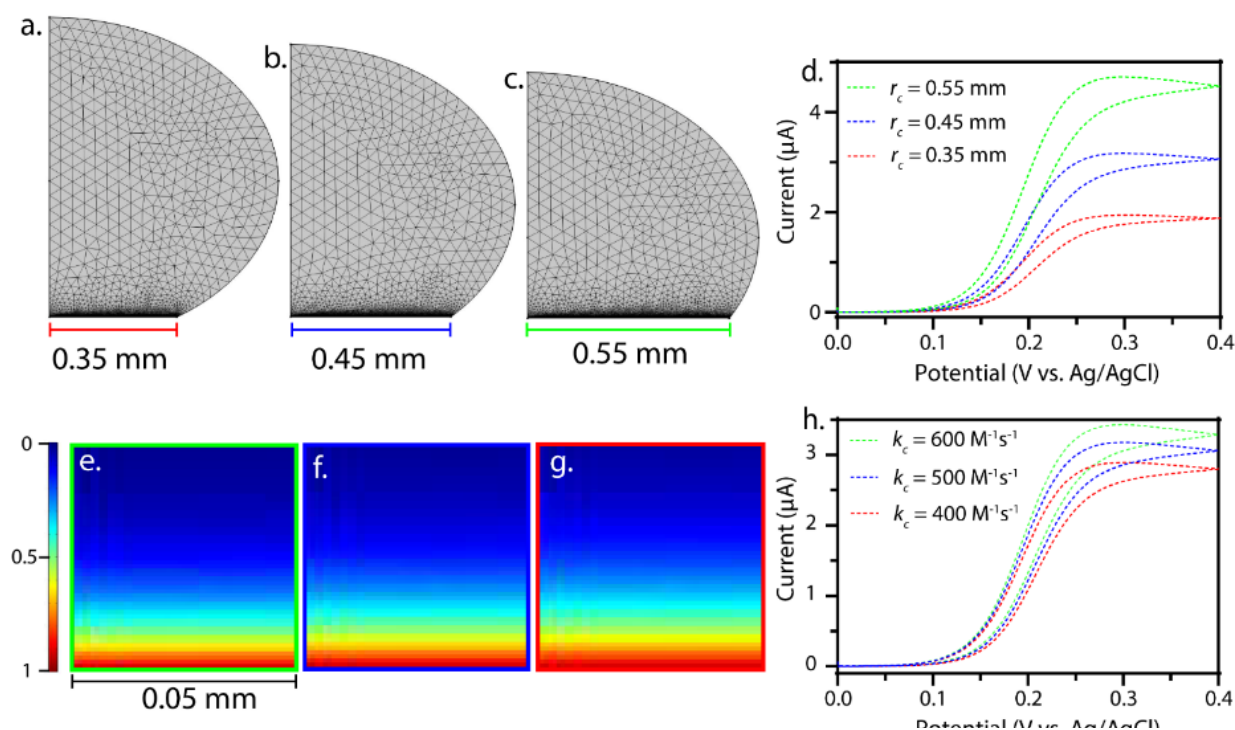


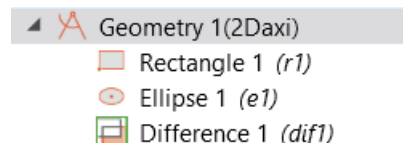
Figure S7. Effect of changing the contact radius. (a-c) Geometry and mesh for a droplet with a contact of 0.35 mm (a), 0.45 mm (b), and 0.55 mm (c). (d) Overlaid simulated voltammograms for the reaction of 1 mM hexacyanoferrate (II) and 10 mM cysteine, where the scan rate for all simulations was 0.05 V/s, and the geometry was changed as shown in a-c. **Effect of changing the k_c parameter.** (e-g) The concentration profile (0 – 1 mM) for hexacyanoferrate (III) 8 s (corresponding to ~ 0.4 V) into the voltammetry where the contact radius = 0.45 mm and $k_c = 600 \text{ M}^{-1}\text{s}^{-1}$ (e), $k_c = 500 \text{ M}^{-1}\text{s}^{-1}$ (f), and $k_c = 400 \text{ M}^{-1}\text{s}^{-1}$ (g). (h) Overlaid simulated voltammograms for the reaction of 1 mM hexacyanoferrate (II) and 10 mM cysteine, where the k_c parameter is 400 (red), 500 (blue), and 600 (green). The scan rate for all simulations was 0.05 V/s. In line with IUPAC convention the anodic current is plotted as positive.

COMSOL Simulation with Adsorption.

COMSOL Multiphysics 5.6 was used to develop a model that accounts for cysteine adsorption to the liquid|liquid boundary.

Geometry and mesh

The geometry was built by a 2D-axisymmetric model, where the droplet was defined as a 90° sector angle of an ellipse with radii determined from microscopy. Some of the droplet height was subtracted from the bottom to create an electrode surface in contact with the droplet (see right for graphics and below for model builder).



Free triangular mesh in three sizes (defined by maximum element size) was used for the domain (10 μm), droplet boundary (1 μm) and electrode boundary (0.1 μm).

Physics

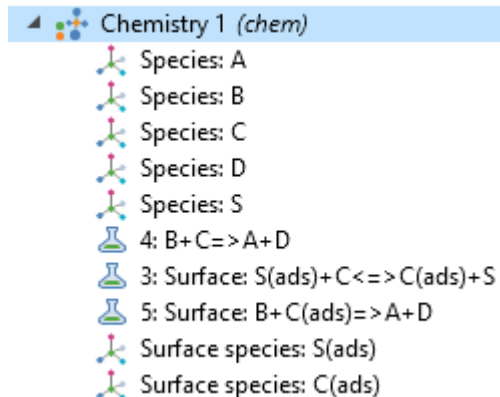
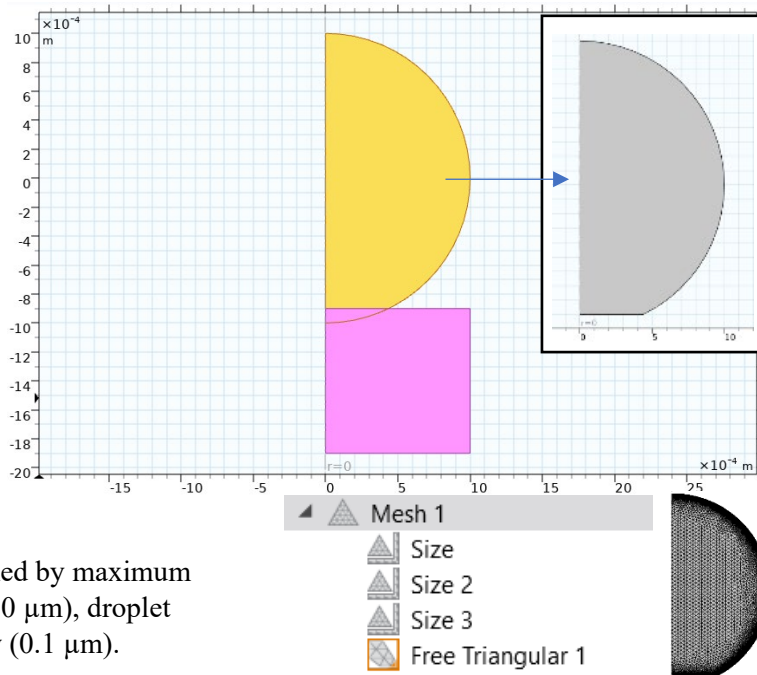
Chemistry

Adsorption is modeled by surface equilibrium reactions at the liquid|liquid boundary. Throughout this model, “A” denotes hexacyanoferrate(II) (ferrocyanide, Fo) “B” denotes hexacyanoferrate(III) (ferricyanide, Fi), “C” denotes cysteine, and “S” is a binding site. Only cysteine adsorption is considered in detail, with an equilibrium constant, $K_{eq} = 1000$. The equilibrium equation was described as a reversible reaction, where the forward (adsorption) rate = $0.1 \text{ M}^{-1}\text{s}^{-1}$ and the backward (desorption) rate was $0.0001 \text{ M}^{-1}\text{s}^{-1}$. This yields the same result as defining the reaction as an equilibrium reaction, but in our experience, allows for better convergence when parameters are changed. Electrostatics are not considered.

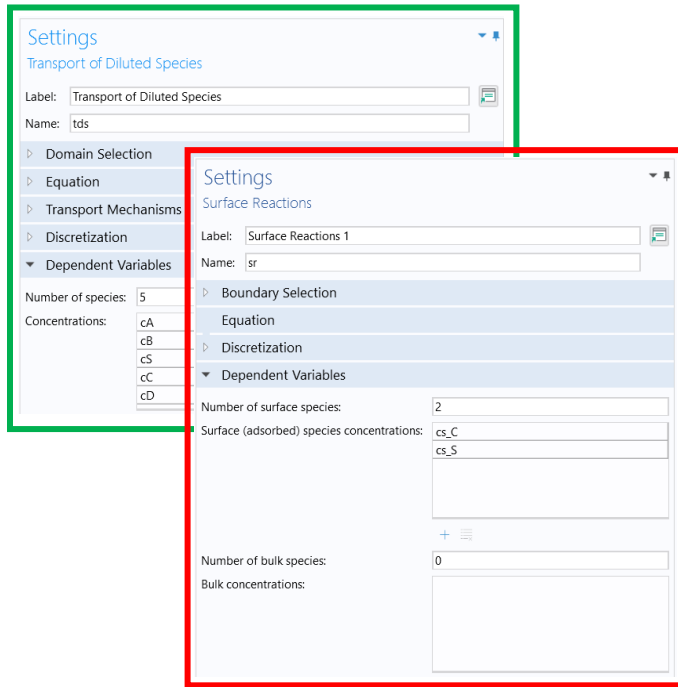
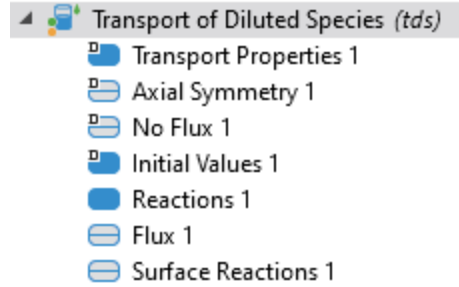
The bimolecular reaction between hexacyanoferrate(III) and cysteine is assumed to be an irreversible reaction with a bimolecular rate of $309 \text{ M}^{-1}\text{s}^{-1}$ (the average kinetic value determined by fitting cyclic voltammograms in bulk, continuous water). We do not consider the dimerized product, cystine, in this model.

Transport of Diluted Species

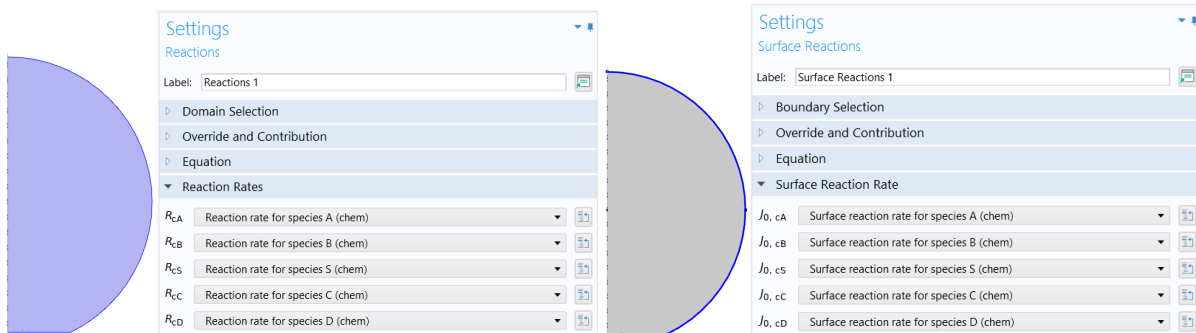
The species within the droplet are governed by “Transport of Diluted Species” physics. Here we describe the concentrations and diffusion of the free species (see parameter list below for values). In these simulations, the only transport mechanism considered is diffusion. There are four reactions occurring



simultaneously: the electrochemical oxidation of hexacyanoferrate(II) to hexacyanoferrate(III), the chemical regeneration of hexacyanoferrate (II) by cysteine oxidation, the equilibrium reaction for the adsorption and desorption of cysteine, and the chemical regeneration of hexacyanoferrate (II) by surface (adsorbed) cysteine oxidation. The bulk (not adsorbed) species are matched between the Chemistry and Transport of Diluted Species (tds) physics in the Chemistry settings (green boxes below) and the surface (adsorbed) species are matched between the Chemistry and Surface Reactions (sr) physics.



The adsorption reactions described in the Chemistry physics are linked to the Transport of Diluted Species physics (tds) by a surface reaction boundary condition. Here, the reaction conditions for each bulk (not adsorbed) species are referenced both in the droplet and at boundary.



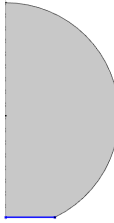
The electrochemical reaction $cA(\text{Fo}) \leftrightarrow cB(\text{Fi})$ is defined in the Transport of Diluted Species physics as a flux boundary condition at the electrode surface. We used the Butler-Volmer formalism for heterogeneous reactions, where the flux of A and B are dependent on the overpotential (η).

Inward Flux

Flux type:
General inward flux

Species cA
 $J_{0,cA} = k_0 \cdot (c_B \cdot \exp(-\alpha) \cdot f(\eta)) - c_A \cdot \exp((1-\alpha) \cdot f(\eta))$ mol/(m²·s)

Species cB
 $J_{0,cB} = -k_0 \cdot (c_B \cdot \exp(-\alpha) \cdot f(\eta)) - c_A \cdot \exp((1-\alpha) \cdot f(\eta))$ mol/(m²·s)



We are studying rates *via* voltammetry, where the applied potential changes as a function of time while current is measured. This function is described as an interpolation creating a triangular sweep through potentials (green boxes). A variable is created to take the difference of the applied potential (relative to time) and the equilibrium potential of the electrochemical reaction ($ET(t) - E_f$) and is named ‘eta’ (red boxes).

Component 2 (comp2)

- Definitions
 - Variables 1
 - Interpolation 1 (ET)

Variables

| Name | Expression | Unit |
|------|---------------|------|
| eta | $ET(t) - E_f$ | V |

Settings

Interpolation

Plot Create Plot

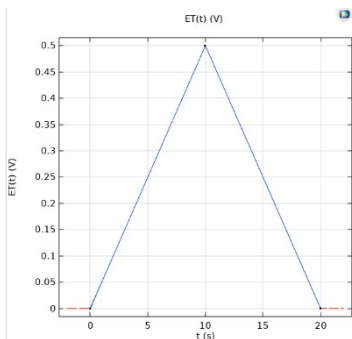
Label: Interpolation 1

Definition

Data source: Local table

Function name: ET

| t | f(t) |
|------|------|
| 0 | Ei |
| ts | EF |
| 2*ts | Ei |



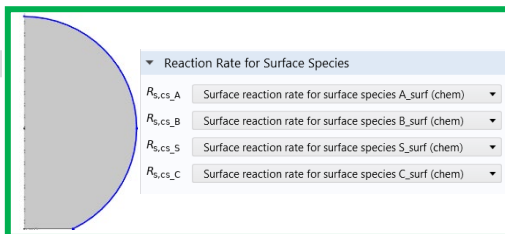
The species on the droplet surface are governed by Surface Reactions physics, where the concentrations and diffusion of the adsorbed species are described. For this model, we assume there is no diffusion along the boundary. We describe a density of sites as G_0 , where this value estimates a highly dense monolayer, assuming a small surface area that a molecule might occupy, a 0.1 nm x 0.1 nm square, and assumes a monolayer on the droplet surface (density of sites = $\sim 2 \times 10^{-4}$ mol/m²). Our model does not account for ionic or intermolecular interactions. The adsorbed species are matched to the surface species in the Chemistry physics (shown above). The reaction rate conditions for each surface (adsorbed) species are described in the Chemistry equations are referenced in the “Reactions.”

Surface Reactions 1 (sr)

- Surface Properties 1
- No Flux 1
- Axial Symmetry 1
- Initial Values 1
- Reactions 1

Reaction Rate for Surface Species

- $R_{s,c_s,A}$ Surface reaction rate for surface species A_surf (chem)
- $R_{s,c_s,B}$ Surface reaction rate for surface species B_surf (chem)
- $R_{s,c_s,S}$ Surface reaction rate for surface species S_surf (chem)
- $R_{s,c_s,C}$ Surface reaction rate for surface species C_surf (chem)



Validation of reaction components

1. Adsorption

Adsorption is dictated by surface equilibrium reactions at a boundary. One way to validate this is to compute the surface coverage as a function of bulk concentration, a plot that should resemble a binding isotherm. The general equation for a Langmuir isotherm is given below:

$$\theta = \frac{K_{ads}c_A}{1+K_{ads}c_A}$$

where θ is the surface coverage of a species, K_{ads} is the equilibrium constant for adsorption, and c_A is the concentration of a species. Figure S8a shows a binding isotherm for cysteine surface coverage *versus* bulk concentration. Figure S8b shows that the species in the droplet reach equilibrium very quickly and fill all of the binding sites (see parameter list below).

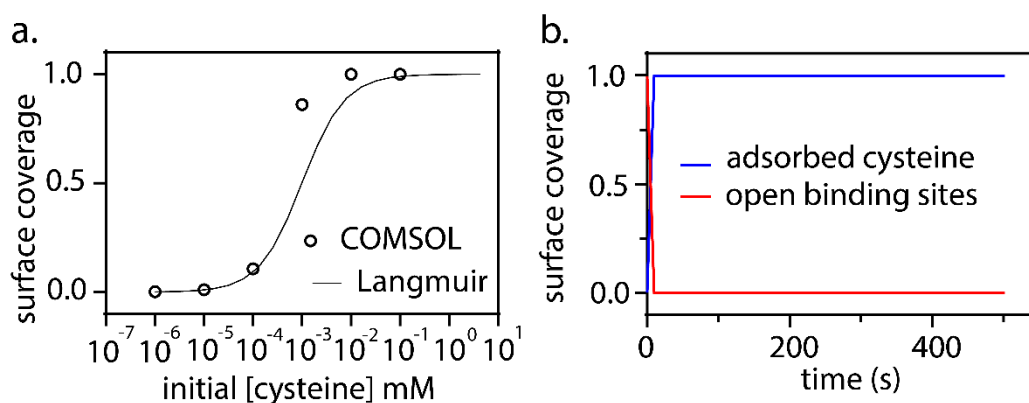


Figure S8. (a) Binding curve plotting the surface coverage of cysteine (C) over the log of the initial droplet concentrations, where the surface density was 2×10^{-7} mol/m² and $K_{eq} = 1000$. (b) Plot of surface coverage as a function of time for 10 mM cysteine (blue line) and free binding sites (red line) for a surface density of 2×10^{-4} mol/m². These data could be obtained from any point on the liquid|liquid interface but were chosen at the droplet equator.

2. Electrochemistry

The electrochemistry is modeled by Butler-Volmer kinetics describing a flux boundary condition at the electrode surface. Plots of current *vs.* potential are generated by describing two “Derived Values” in the Results section. A “Global Evaluation” of ET(t) yields the time-dependent potential (red boxes), and the current is solved as a line integration over the electrode boundary, where the flux is multiplied by Faraday’s constant to give amperes (green boxes).

| Derived Values | |
|-----------------|------|
| (*) Potential | |
| Current | |
| » Expression | Unit |
| ET(t) | V |
| » Expression | Unit |
| tds.ntflux_cA*F | A |

Cyclic voltammograms of the electrochemical reaction of 1 mM hexacyanoferrate(II) in the droplet with and without adsorption of cysteine were simulated. Figure S9a shows the geometry and reactions included in these simulations. Figure S9b indicates that the adsorption equilibrium under these conditions does not largely influence the voltammetry.

For voltammetry without the follow-up chemical reaction, we compared the simulated peak current for the droplet shown in Figure S9a to the peak current predicted by the Randles-Sevcik equation. Figure S9b shows a peak current (i_p) of 0.98 μA , which has good agreement with the peak current predicted by the Randles-Sevcik equation ($i_p = 0.92 \mu\text{A}$) shown below,

$$i_p = 268600 n^{\frac{3}{2}} A D^{\frac{1}{2}} C v^{\frac{1}{2}}$$

where n is the number of electrons (1), A is the electrode area ($0.60 \mu\text{m}^2$), D is the diffusion coefficient ($6.5 \times 10^{-10} \text{ m}^2/\text{s}$), C is the concentration of hexacyanoferrate(II) (1 mM), and v is the scan rate (0.05 V/s).

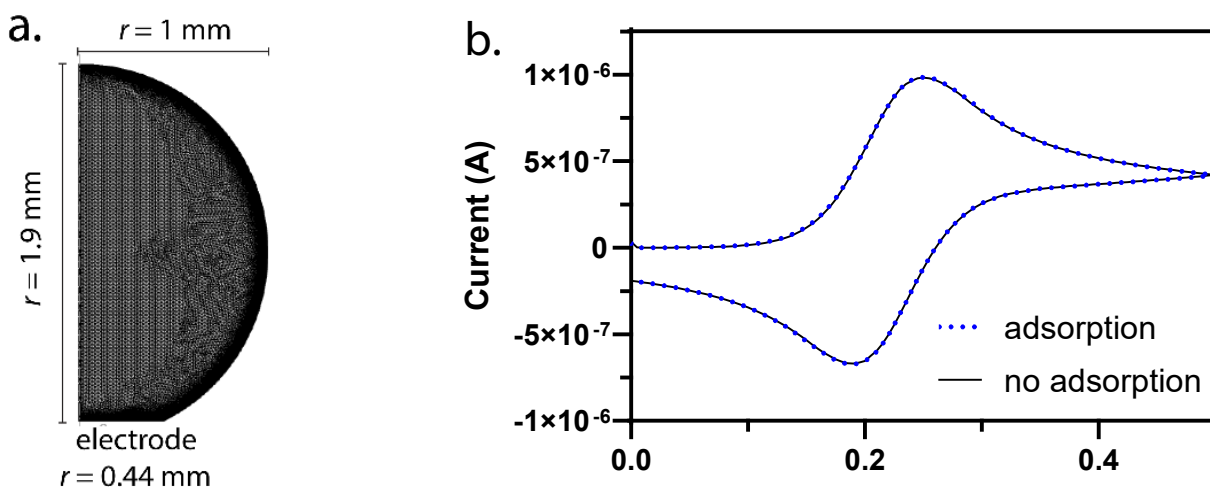


Figure S9. (a) 2D axisymmetric geometry used for the simulation. (b) Simulated cyclic voltammograms for 1 mM hexacyanoferrate(II) with (blue dotted line) and without (solid black line) cysteine. It should be noted that this voltammetry is simulated without the follow-up chemical reaction between hexacyanoferrate (III) and cysteine. The scan rate was 50 mV/s. See parameter list for more details.

3. Simultaneous adsorption, electrochemical, and chemical reactions

The chemical reaction for cysteine oxidation is introduced as an irreversible reaction in the bulk domain. Figure 4b in the main text shows that general EC' voltammetric character is observed with and without adsorption. Please see the associated GIF file to observe how cysteine adsorption changes as a function of distance from the electrode with respect to time during these experiments. In this GIF, the y-axis is surface coverage of cysteine. The x-axis is the distance from the electrode ($x = 0$) along the liquid|liquid boundary. Importantly, the surface coverage of cysteine covers to 1, as in the adsorption-only model at distances far from the electrode. The coverage is dynamic for points close to the electrode as here the concentration profiles change with respect to potential/time.

Table S4. Simulation Parameters (adsorption simulation)

| Name | Expression/Value | Description |
|---------|---|---|
| ra | Informed by photo [mm] | height of droplet |
| rb | Informed by photo [mm] | width of droplet |
| rb | Informed by photo [mm] | contact radius of droplet |
| k_f | 0.1 | adsorption rate constant for all adsorption |
| k_b | 0.0001 | desorption rate constant for all adsorption |
| G0 | 2E-4 mol/m ² | total binding site density |
| v | 0.05 [V/s] | scan rate |
| ts | abs(EF-Ei)/v | sweep time |
| T | 293.15[K] | temperature |
| SD_S | 1E-9 [m ² /s] | BS surface diffusion constant |
| SD_C | 1E-9 [m ² /s] | cysteine surface diffusion constant |
| SD_B | 6.5E-10 [m ² /s] | hexacyanoferrate (III) surface diffusion constant |
| SD_A | 6.5E-10 [m ² /s] | hexacyanoferrate (II) surface diffusion constant |
| sconc_C | 0 [mol/m ²] | initial concentration of surface cysteine |
| sconc_B | 0 [mol/m ²] | initial concentration of surface hexacyanoferrate (III) |
| sconc_A | 0 [mol/m ²] | initial concentration of surface hexacyanoferrate (II) |
| sconc_S | 2E-4 [mol/m ²] | initial concentration of surface sites |
| R2 | 8.314 [J/K/mol] | gas constant |
| n | 1 | number of electrons hexacyanoferrate (II/III) |
| k0 | 1 [cm/s] | heterogenous rate hexacyanoferrate (II/III) |
| k_c | 309 [M ⁻¹ *s ⁻¹] | bimolecular rate |
| F | 96485 [C/mol] | Faraday's constant |
| f | F/(R2*T) | constant |
| Ei | 0 [V] | initial potential |
| EF | 0.5 [V] | final potential |
| Ef | 0.21 [V] | equilibrium potential hexacyanoferrate (II/III) |
| D_S | 1E-9 [m ² /s] | BS diffusion coefficient |
| D_C | 1E-9 [m ² /s] | cysteine diffusion coefficient |
| D_B | 6.5E-10 [m ² /s] | hexacyanoferrate (III) diffusion coefficient |
| D_A | 6.5E-10 [m ² /s] | hexacyanoferrate (II) diffusion coefficient |
| conc_S | 0 [mM] | initial bulk concentration of binding sites |
| conc_C | 5 [mM] | initial bulk concentration of cysteine |
| conc_B | 0 [mM] | initial bulk concentration of hexacyanoferrate (III) |
| conc_A | 0.5 [mM] | initial bulk concentration of hexacyanoferrate (II) |
| alpha | 0.5 | charge transfer coefficient hexacyanoferrate (II/III) |

References

1. Moldenhauer, J.; Meier, M.; Paul, D. W., Rapid and Direct Determination of Diffusion Coefficients Using Microelectrode Arrays. *Journal of The Electrochemical Society* **2016**, *163* (8), H672-H678.
2. Wang, S.-f.; Du, D.; Zou, Q.-C., Electrochemical behavior of epinephrine at l-cysteine self-assembled monolayers modified gold electrode. *Talanta* **2002**, *57* (4), 687-692.
3. Ralph, T. R.; Hitchman, M. L.; Millington, J. P.; Walsh, F. C., The reduction of l-cystine in hydrochloric acid at mercury drop electrodes. *Journal of Electroanalytical Chemistry* **2006**, *587* (1), 31-41.
4. Research, D. Diffusion Coefficients. <https://www.dgtresearch.com/diffusion-coefficients/>.
5. Bard, A. J., Elements of Molecular and Biomolecular Electrochemistry: An Electrochemical Approach to Electron Transfer Chemistry By Jean-Michel Savéant (Université de Paris 7, Denis Diderot). J. Wiley & Sons, Inc.: Hoboken, NJ. 2006. xviii + 486 pp. \$135. ISBN 0-471-44573-8. *J Am Chem Soc* **2007**, *129* (1), 242-242.